Journal of Physics: Conference Series **326** (2011) 012057 doi:10.1088/1742-6596/326/1/012057

Conventional and 360 degree electron tomography of a micro-crystalline silicon solar cell

M Duchamp[1], A Ramar[1], A Kovács[1], T Kasama[1], F-J Haug[2], SB Newcomb[3], C Ballif[2] and RE Dunin-Borkowski[4-1]

[1] Center for Electron Nanoscopy, Technical University of Denmark, DK-2800 Kongens Lyngby, Denmark

[2] Photovoltaics and Thin Film Electronics Laboratory, Ecole Polytechnique Fédérale de Lausanne, Rue Breguet 2, CH-2000 Neuchâtel, Switzerland

[3] Glebe Laboratories, Newport, Co. Tipperary, Ireland

[4] Institute for Microstructure Research, Forschungszentrum Jülich, D-52425 Jülich, Germany

E-mail: martial.duchamp@cen.dtu.dk

Abstract. Bright-field (BF) and annular dark-field (ADF) electron tomography in the transmission electron microscope (TEM) are used to characterize elongated porous regions or cracks (simply referred to as cracks thereafter) in micro-crystalline silicon (μc-Si:H) solar cell. The limitations of inferring the 3D geometry of a crack from a tilt series of images acquired from 100-nm-thick focused ion beam (FIB) milled TEM specimen are discussed. In an attempt to maximize the specimen tilt range and to reduce the effects of diffraction and phase contrast on the reconstruction, both BF and ADF electron tomography are used to acquire 360º tilt series of images from a FIB-prepared needle-shaped μc-Si:H specimen.

1. Introduction

Thin film microcrystalline silicon (μc-Si:H), prepared by plasma-enhanced chemical vapour deposition, is a promising material for use as the active absorber layer in low cost solar cells [1], for which efficiencies higher than 8% have been obtained on flexible substrates [2] and over 10% on glass substrates [3], with higher efficiencies when used in tandem solar cells based on a stack of a-Si:H and μc-Si:H cells. The use of rough substrates has been demonstrated to increase light trapping efficiency and overall solar cell efficiency [4]. However, the presence elongated porous regions (called cracks thereafter) between adjacent agglomerations of nanocrystals is thought to decrease electrical performance, as they can introduce shunts between the top and bottom contacts, thereby decreasing the open-circuit voltage and the fill-factor of the solar cell [5].

Transmission electron microscopy (TEM) combined with electron tomography is a suitable technique for the analysis of the redistribution of different materials in a three-dimensional volume. However, the detection of a region of lower density within a crystalline matrix using electron tomography is still challenging [6], even if the requirement that the recorded image intensity should be

a monotonic function of a desired property proportional, e.g. specimen thickness or chemical composition, is approximately justified by acquiring annular dark-field (ADF) images, which are less sensitive to diffraction contrast than conventional bright-field (BF) images.

Here, we assess the applicability of both BF and ADF electron tomography reconstruction of (i) a crack in a μc-Si:H matrix and (ii) fine-grained Si nanocrystals in a needle-shaped sample in which missing wedge artifacts are reducing by allowing images to be acquired as the specimen is tilted through 360º in the TEM [7].

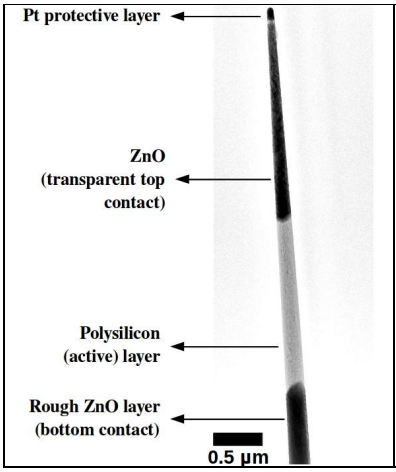

Figure 1. Bright-field TEM image of a needle-shaped μc-Si:H solar cell specimen prepared for 360º electron tomography using focused ion beam milling. Diffraction contrast in the Si layer is averaged other the CCD camera pixels due to the low magnification mode.

2. Experimental details

The solar cell samples examined here were grown onto pyramidal ZnO surface textures that had been deposited by low-pressure chemical vapour-deposition processes onto glass substrates [8]. Single-junction thin-film μc-Si:H layers were grown in the form of n-i-p sequences using plasma-enhanced chemical vapour deposition under standard conditions of plasma power, temperature and silane flux (4 W, 200 °C and 7.3 sccm, respectively).

TEM specimen preparation of thin film silicon solar cells can be highly challenging since they are made on plastic, glass or metallic substrates. Here, both conventional 100-nm-thick lamellar and 200-nm-diameter needle-shaped specimens (Figure 1) were prepared using focused ion beam (FIB) milling in a dual-beam FEI Helios microscope. Tilt series of BF TEM images were acquired in an FEI Tecnai T20 TEM, while tilt series of ADF scanning (S)TEM images were acquired in an FEI Titan TEM, using 47.4 and 10.2 mrad inner ADF detector semi-angles for crack and polysilicon characterization, respectively. All measurements were carried out at 120 keV to minimize electron beam damage. Each tilt series of images was aligned manually due to the limited number of recognizable specimen figures. Tomographic reconstructions were performed using the simultaneous iterative reconstruction technique (SIRT) algorithm with 30 iterations using FEI Inspect3D software.

3. Results and discussion

3.1. Crack characterization in a conventional TEM lamella

Figure 2 (a) shows a tomographic reconstruction of a crack in μc-Si:H obtained from (a) BF TEM image series acquired from a conventional 100-nm-thick FIB-prepared TEM lamella using a tilt range of ±60º. The growth direction of the μc-Si:H layer is the *y*-direction. The crack is visible in the form of a region of reduced density close to the centre of the volume. Similar contrast at the edge of the reconstructed volume is an artefact that may have resulted from the limited tilt range. In Fig. 2 (a), the approximate shape of the crack is recovered, but its precise lateral dimensions are likely to be in error

as a result of the effect of local variation in diffraction contrast in the μc-Si:H matrix on the reconstruction.

Figures 2 (b) and (c) show corresponding results obtained by applying ADF TEM tomography with a tilt range of ±60º. Fig. 2 (b) shows a section through the reconstructed volume in which the crack is shown in grey, the μc-Si:H matrix in red and residual artefacts that may arise from the limited tilt angle in yellow. Figure 2 (c) shows a 3D iso-surface representation of the volume occupied by the crack. The bounding box represents the size of the reconstruction volume in the *y*- and *x*-directions, and a region in the *z*-direction that was selected to remove missing wedge artefacts. The use of a needle-shaped sample that allows a 360º tilt range to remove such artefacts is described below.

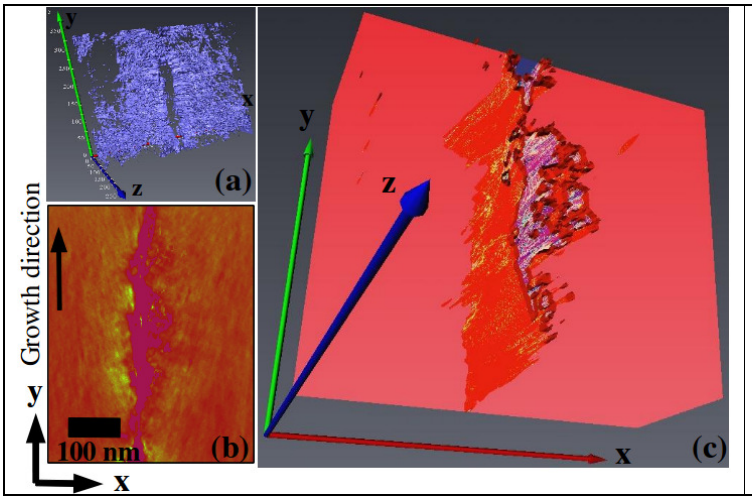

Figure 2. (a) Electron tomographic reconstruction of a crack in μc-Si:H obtained from bright-field TEM tilt series of images. (b-c) Corresponding annular dark-field tomographic reconstruction showing (b) the section through reconstructed volume and (c) an iso-surface representation of the crack volume in a region of the reconstruction that excludes many of the most serious missing wedge artefacts.

3.2. μc-Si:H characterization in a needle-shaped specimen

Figure 3 (a) shows a BF TEM picture of a needle-shaped specimen, taken from a tilt series of images of μc-Si:H acquired over a full 360º tilt range. In Fig. 3 (a), individual crystals are in strongly diffracting orientation and the local growth direction of the μc-Si:H is perpendicular to the ZnO. Fig. 3 (b) shows a section through a reconstructed volume created from the tilt series of images that include Fig. 3 (a). The reconstruction reveals the presence of a 20-nm-thick amorphous layer at the edge of the needle resulting from amorphization of the edge of the μc-Si:H specimen during ion milling. Fig. 3 (c) shows a vortex projection of the reconstructed volume in which the contrast has been affected by diffraction contrast from Si nanocrystals visible in the original BF TEM images in the tilt series.

Figure 3 (d) shows an ADF STEM image of the same needle-shaped sample acquired using an inner semi-angle detector of 47.4 mrad. This image is much less sensitive to diffraction contrast than the BF image shown in Fig. 3 (a) and much more directly interpretable in terms of variations in projected density. Fig. 3 (e) shows a section through the reconstructed volume, in which the darker contrast at the edge of the needle is due to Ga^{2+} implantation during FIB milling. The contrast from the Si nanocrystals in the needle is less pronounced than in Fig. 3 (b) but is still visible. Fig. 3 (f) shows two orthogonal sections through the reconstructed volume.

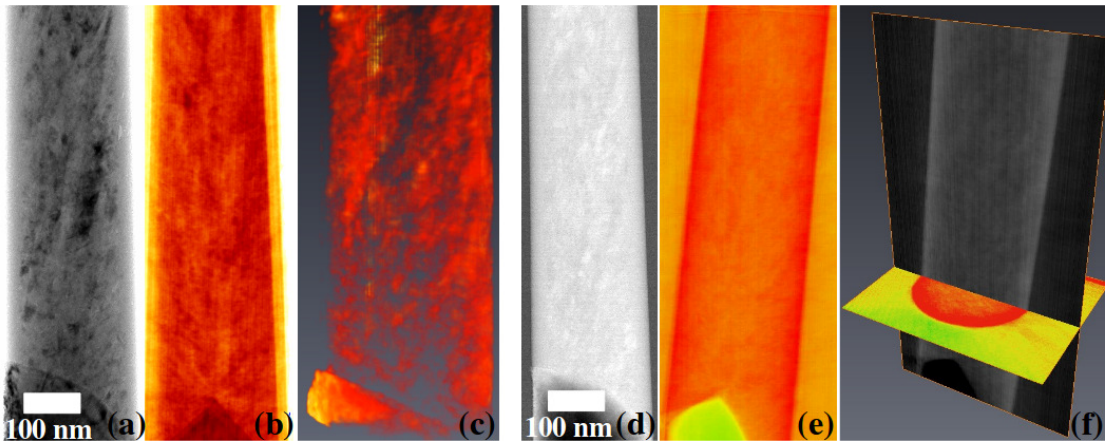

Figure 3. (a) BF TEM image of a 200 nm diameter needle-shaped specimen of μc-Si:H on rough ZnO; from a tomographic tilt series acquired with a tilt range of 360º. (b) shows a section through the reconstructed volume, while (c) shows a vortex projection. (d) ADF image taken from a tilt series of images of the same needle using an inner detector semi-angle of 47.4 mrad. (e) shows a central section while (f) shows two orthogonal sections of the reconstructed volume.

4. Conclusions

Tomographic tilt series of BF and ADF images have been used to obtain three-dimensional reconstructions of μc-Si:H in a thin film solar cell. A reconstruction of a crack in a conventional FIB-prepared lamella shows artefacts resulting from the effect of the limited tilt range used. A needle-shaped sample is used to achieve a 360º tilt range to overcome this problem, although two effects of diffraction contrast and difficulties with image alignment are not eliminated completely. Ongoing work involves addressing these problems and preparing a needle-shaped specimen that contains a single crack within its volume.

References

[1] Shah A, Torres P, Tscharner R, Wyrsch N and Keppner H 1999 *Science* **285** 692
[2] Haug F-J, Soderstrom T, Python M, Terrazzoni-Daudrix V, Niquille X and Ballif C 2009 *Solar Energy Materials and Solar Cells* **93** 884
[3] Yamamoto K, Toshimi M, Suzuki T, Tawada Y, Okamoto T, Nakajima A 1998 *MRS Spring Meeting, San Francisco, April 1998*
[4] Čampa A, Krč J and Topič M 2009 *J. Appl. Phys* **105** 083107
[5] Python M, Vallat-Sauvain E, Bailat J, Domine D, Fesquet L, Shah A and Ballif C 2008 *Journal of Non-Crystalline Solids* **354** 2258
[6] Kübel C, Voigt A, Schoenmakers R, Otten M, Su D, Lee T-C, Carlsson A and Bradley J 2005 *Microscopy and Microanalysis* **11** 378
[7] Midgley P A and Dunin-Borkowski R E 2009 *Nature Materials* **8** 271
[8] Faÿ S, Kroll U, Bucher C, Vallat-Sauvain E and Shah A 2005 *Solar Energy Materials and Solar Cells* **86** 385